THE JOURNAL OF PHYSICAL CHEMISTRY B

Article

pubs.acs.org/JPCB

Terminally Grafted Chain Layers in Oligomer−Monomer Solutions: Predictions from a Density Functional Theory

M. Borówko, S. Sokołowski, and T. Staszewski*

Department for the Modeling of Physico-Chemical Processes, Maria Curie-Skłodowska University, 20-031 Lublin, Poland

ABSTRACT: The structure of grafted chain layers immersed in an explicit solvent consisting of chain molecules is studied using density functional theory. We consider bonded layers built of short grafted chains at a moderate grafting density. We investigate the grafted layers in contact with oligomeric solvents and oligomer−monomer solutions. The chain molecules are freely jointed spherical segments. The substrate is assumed to be inert with respect to the grafted chains. The mobile molecules interact with the surface via Lennard-Jones (9-3) potential. The interactions between mobile chains, monomers, as well as segments of the tethered chains are described by Lennard-Jones (12-6) potential. We discuss how the structure of the grafted chain layer depends on the length of mobile chains and strengths of grafted chain−oligomer, oligomer−substrate, oligomer−oligomer, and oligomer−monomer interactions. We study the impact of mixture composition on the height of the bonded layer for selected model systems. The results are consistent with previous experimental and simulation data.

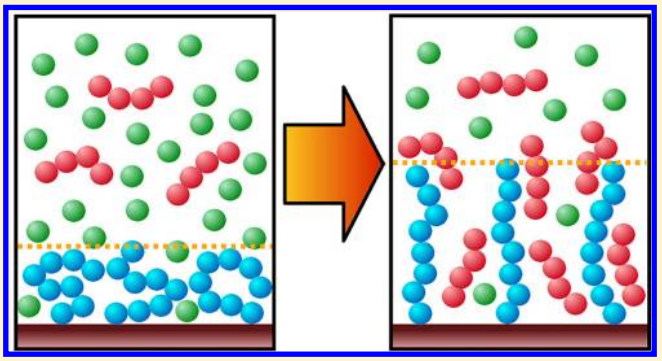

INTRODUCTION

The motivation to study terminally attached polymers is their potential application in such areas as colloidal stabilization, lubrication, chromatographic separation, supported catalysis, drug delivery, and many others. Grafted chains are widely used in surface modification of various materials because of their special properties as biocompatible layers, environmental response materials, and nonfouling coatings. These systems are also very interesting from an academic point of view. Therefore, the end-grafted polymer layers have been studied by numerous groups using a variety of theoretical approaches. Among these are scaling[1,2] and mean-field classical theories,[3,4] self-consistent field methods,[3−22] density functional theory,[22−34] and computer simulations.[27,28,35−46] An overview in the field can be found in several reviews.[47−49]

Scaling theories[1,2] predict in a relatively simple way the correct trends over a variety of conditions. However, they make it possible to obtain only asymptotic power dependencies of thermodynamic characteristics of the system. The main assumption in these models is that all chains are equally stretched with their ends positioned at the same distance from the surface. This is a serious oversimplification, which underestimates the conformational entropy of the grafted chains.

The self-consistent field methods are more rigorous and provide detailed information on the structure of the surface layer. In such models the ends are allowed to distribute themselves throughout the brush.[5−22] The methods are based on finding the probability distribution function of chain conformation from a set of nonlinear equations derived by minimizing the free energy. One can divide these theories into two main classes, namely, analytical self-consistent-field models[5−9] and numerical methods.[10−22]

In the limit of strong chain stretching and infinitely long chains, the self-consistent field equations can be solved analytically.[5−9] It is possible when the set of conformations of the chains is replaced by the most probable trajectory. In these models fluctuations around the classical polymer path are not taken into account. Such fluctuations, however, may affect the structure of the grafted chain layer, especially at low grafting densities or in the case of short grafted chains.[47] The theories do not reproduce correctly the properties of the layer smaller than its height.[9,18] The analytical self-consistent field model predicts a parabolic density profile of the brush.

The numerical self-consistent field methods in various ways include the conformational fluctuations. In these models the local segment density is the sum of local densities of all possible chain conformations, weighted by the probability of each conformation. On the other hand, the conformation probability depends on the distribution of the total density. This density profile is determined numerically. It is found that the conformational fluctuations may result in an extended tail region, in which the segment density of grafted chains smoothly decreases to zero. The lattice version of the self-consistent field theory formulated by Scheutjens and Fleer[50,51] for the adsorption of homopolymers has gained considerable popularity because of a simplicity of numerical implementation. This approach has been also extended to the grafted chain layers and

Received: March 20, 2013
Revised: August 14, 2013

   dx.doi.org/10.1021/jp4027546 | J. Phys. Chem. B XXXX, XXX, XXX−XXX

used to investigate various bonded phases.[10−16] A further progress in the theory of polymeric fluids was attained due the single-chain mean-field method proposed by Carignano and Szleifer.[19−22] Within this approach the configuration statistics of a chosen chain are described exactly, whereas the interactions with the molecules of the environment are calculated in the framework of a mean-field approximation. The numerical self-consistent field theories were compared with classical mean-field models by Netz and Schick.[18]

The end-grafted chains have also been studied using several versions of the density functional theory.[23−34] McCoy and co-workers[23] proposed the density functional theory to study end-grafted polymer layers both in the presence of a solvent and in "a continuum-solvent" approximation. Using the Flory−Huggins theory as input, they showed that their approach reduces to the self-consistent field theory. Another version of the density functional theory was developed by Yu and Wu.[52,53] This method has been used to study adsorption of various molecules on the modified surfaces[27−34] and structural changes in the polymer layers connected with the adsorption.[32,33] Among different theoretical approaches devised to study polymeric fluids at interfaces, the numerical self-consistent field theory and the density functional theory have attracted considerable interest in recent years. The relations between these theories have been discussed, and it has been proved that they are essentially equivalent.[54−56] A detailed analysis of differences is beyond the scope of this paper. It is worth stressing that both theories may be used to describe distinct grafted chain layers because they do not introduce any general assumptions connected with the chain length, the grafting density, or a degree of chain stretching.

The most detailed studies of the theoretical problem in question have been done by performing computer simulations, using Monte Carlo[27,28,35,40−44] and molecular dynamics[36−39,45,46] methods. The main objective of many simulations was to test the validity of the self-consistent field theory. Molecular simulations have also been used to study various problems connected with applications of the polymer brushes, such as modification of the surface wettability[40] and the retention in chromatography with the chemically bonded phases.[43−46]

The properties of the polymer layer depend on numerous factors including type of grafted molecule (linear or branched, homogeneous or containing polar functional groups), type of substrate, solvent quality, grafting density, composition of the mixed solvent, etc. A good tool for the reversible modeling of the structure of the bonded phase is an optimal choice of a solvent. The problem of the solvent-induced structural rearrangement of the grafted chain layer has been explored in the framework of different theoretical models.[47−49]

A series of theoretical investigations have been devoted to grafted chains immersed in mixed solvents.[4,7−9] The mean-field theory of terminally anchored chains of finite extensibility has been proposed by van Zatten.[4] In this approach the polymer layer was described in the framework of the Alexander model.[1] He has considered mixed polydisperse solvents of varying quality. The analytical self-consistent field theory has been developed by Zhulina et al.[8] for the tethered chain layer immersed in a solution of mobile chains that were considerably shorter than the grafted polymers. The theory of this kind has been also applied to study the grafted chains in multi-component solvents.[9] The authors concentrated on binary solvents with partially miscible components and possible phase transitions. Martin and Wang[17] have used the numerical self-consistent field theory to study interbrush penetration in mixed solvents. Because these theories involved some restricting assumptions they did not predict a proper structure of the surface layer; for example, they are lacking in short-scale description, such as oscillatory density profiles. In our previous papers[30,31,33] we have used the density functional theory to investigate adsorption on the grafted layers in contact with mixtures of small molecules. The resulting segment density profiles exhibited an oscillatory behavior that is in accord with computer simulations.[27,28]

One of the most important applications of the grafted chain layers is chromatography. In this method adsorbents with chemically bonded polymer chains are used as stationary phases (so-called chemically bonded phases). The most popular packings of chromatographic columns are built of short alkyl chains, consisting of 4, 8, 18, or 30 methylene groups. In the separation process binary mixtures of different solvents are usually applied as mobile phases. Because of the great practical importance of chromatography, such bonded phases in contact with liquid mixtures have been investigated experimentally using the nuclear magnetic resonance,[57,58] fluorescence,[59] vibrational,[60] and Raman[61,62] spectroscopy. Much effort has also been directed toward theoretical description of the chromatographic systems.[29,63] The effect of the stationary phase structure on the solute retention has been studied using computer simulations.[36,43−46] Unfortunately, the molecular simulations can be carried out for a few systems only. The scanning of the space of the parameters, which affect the properties of the bonded phase, would be very time-consuming. However, the density functional theory allows us to perform such model calculations for numerous sets of parameters.

In this paper we deal with short grafted chains immersed in a binary solution. We consider the model systems similar to those used in liquid chromatography. The major goal of the study is to answer the question how the thickness of the grafted chain layer changes with the solvent composition. We analyze the impact of size of solvent molecules on the properties of the grafted layer. The role of solid−solvent, grafted chain−solvent, and solvent−solvent interactions is also considered.

The outline of the paper is as follows. In Section II the model and the computational methods are briefly described. Section III presents our results and the analysis. Finally, we summarize the conclusions in Section IV.

THEORY

We study end-grafted chains in contact with a monomer−oligomer solution. The system consists of tethered chains (P), free chains (1), and spherical monomers (2). We employ a simple model of the system that was used in previous work.[31] According to this model, the chains are represented by tangentially jointed M_k spherical beads of the same diameter, $\sigma^{(k)} = \sigma$. The chain connectivity is enforced by the bonding potential

$$\exp[-\beta V_B(\mathbf{R})] = \prod_{i=1}^{M_k-1} \delta(|\mathbf{r}_{i+1} - \mathbf{r}_i| - \sigma^{(k)})/4\pi(\sigma^{(k)})^2 \quad (1)$$

where k = P, 1; $\mathbf{R}_k \equiv (\mathbf{r}_1, \mathbf{r}_2, ..., \mathbf{r}_{M_k})$ is the vector specifying positions of segments; the symbol δ denotes the Dirac function; and $\beta^{-1} = k_B T$.

dx.doi.org/10.1021/jp4027546 | J. Phys. Chem. B XXXX, XXX, XXX−XXX

Each tethered chain (P) contains one surface-binding segment, located at its end (the segment number 1) that interacts with the wall via the bonding, V_b, potential

$$\exp[-\beta v_{s1}^{(P)}(z)] = C\delta(z - \sigma^{(P)}/2) \quad (2)$$

where z is a distance from the surface and C is a constant. The potential (2) implies that the surface-binding segments lie at the distance $z_0 = \sigma^{(P)}/2$ from the wall. The remaining segments of the grafted chains interact with the surface via the hard-wall potential. However, the segments of free molecules interact with the surface via the Lennard-Jones (9-3) potential

$$v^{(k)}(z) = \varepsilon_s^{(k)}[(z_0^{(k)}/z)^9 - (z_0^{(k)}/z)^3] \quad (3)$$

where $\varepsilon_s^{(k)}$ is the energy parameter that characterizes the strength of interaction between the kth component and the solid surface ($\varepsilon_s^{(k)} = -(9/8)^{1/3}\nu_{min}^{(k)}$, $\nu_{min}^{(k)}$ is the value of the potential (3) at a minimum) and $z_0^{(k)} = \sigma^{(k)}/2$.

All segments interact by means of truncated Lennard-Jones (12-6) potential

$$u^{(kl)}(r) = \begin{cases} 4\varepsilon^{(kl)}[(\sigma^{(kl)}/r)^{12} - (\sigma^{(kl)}/r)^6] & r < r_{cut}^{(kl)} \\ 0 & \text{otherwise} \end{cases} \quad (4)$$

where $\varepsilon^{(kl)}$ characterizes interactions between species k and l; $\sigma^{(kl)} = 0.5(\sigma^{(k)} + \sigma^{(l)})$ (k = P,1,2); r is the distance between interacting segments; and r_{cut} is the cutoff distance. In our study $r_{cut} = 3\sigma^{(kl)}$.

We use the Weeks−Chandler−Anderson method[64] to divide the potential (4) into the repulsive (reference)

$$u_{rep}^{(kl)}(r) = \begin{cases} \infty & r < \sigma^{(kl)}2^{1/6} \\ 0 & \text{otherwise} \end{cases} \quad (5)$$

and the attractive (perturbation) part

$$u_{att}^{(kl)}(r) = \begin{cases} -\varepsilon^{(kl)} & r < 2^{1/6}\sigma^{(kl)} \\ u^{(kl)}(r) & r \geq 2^{1/6}\sigma^{(kl)} \end{cases} \quad (6)$$

The theory is constructed in terms of densities of all components, $\rho^{(k)}$, local densities of segments, $\rho_s^{(k)}$, and densities of particular segments of chains, $\rho_{s,i}^{(k)}$, defined as

$$\rho_s^{(k)}(\mathbf{r}) = \sum_{i=1}^{M_k} \rho_{s,i}^{(k)}(\mathbf{r}) = \sum_{i=1}^{M_k} \int d\mathbf{R}\delta(\mathbf{r} - \mathbf{r}_i)\rho^{(k)}(\mathbf{R}) \quad (7)$$

Obviously, for the monomeric solvent $\rho_s^{(2)} = \rho^{(2)}$.

The surface density of grafted chains, i.e., the number of chain molecules per area of the surface (ρ_p), is fixed

$$\int dz\rho_{s,i}^{(P)}(z) = \rho_P \quad (8)$$

The thermodynamic potential of the system under consideration is given by

$$Y = F[\rho^{(P)}(\mathbf{R}_P), \rho^{(1)}(\mathbf{R}_1), \rho^{(2)}(\mathbf{R}_2)] + \int d\mathbf{R}_P\rho^{(P)}(\mathbf{R}_P)v^{(P)}(\mathbf{R}_P) + \sum_{k=1,2}\int d\mathbf{R}_k\rho^{(k)}(\mathbf{R}_k)(v^{(k)}(\mathbf{R}_k) - \mu^{(k)}) \quad (9)$$

where $F[\rho^{(P)}(\mathbf{R}_P), \rho^{(1)}(\mathbf{R}_1), \rho^{(2)}(\mathbf{R}_2)]$ is the free energy functional.

As usual, this functional is expressed as the sum: $F = F_{id} + F_{ex} = F_{id} + F_{hs} + F_c + F_{att}$. The ideal contribution is calculated exactly. The excess free energy due to hard-sphere interactions, F_{hs}, results from the fundamental measure theory of Rosenfeld.[65] The term describing chain connectivity follows from the first-order perturbation theory of Wertheim.[66] The mean-field approximation is used to obtain the free energy due to attractive interactions between fluid molecules

$$F_{att} = \frac{1}{2}\sum_{k=P,1,2}\int d\mathbf{r}_1 d\mathbf{r}_2\rho_s^{(k)}(\mathbf{r}_1)\rho_s^{(k)}(\mathbf{r}_2)u^{(kk)}(\mathbf{r}_{12}) + \frac{1}{2}\sum_{k,l=P,1,2;k\neq l}\int d\mathbf{r}_1 d\mathbf{r}_2\rho_s^{(k)}(\mathbf{r}_1)\rho_s^{(l)}(\mathbf{r}_2)u^{(kl)}(\mathbf{r}_{12}) \quad (10)$$

The minimization of the thermodynamic potential leads to a set of Euler−Lagrange equations for density profiles of all components. In our model these profiles are functions only of the distance from the surface, $\rho_s^{(k)} = \rho_s^{(k)}(z)$. The set of equations is solved by means of the standard numerical iterative method.

In this work we focus our attention on the thickness of the grafted layer defined as[32]

$$h = 2\frac{\int dzz\rho_s^{(P)}(z)}{\int dz\rho_s^{(P)}(z)} \quad (11)$$

We also introduce the normalized height of the grafted chain layer $h^* = h/M_P$.

In previous papers[32,33] we have shown that the height of the grafted chain layer depends on adsorption of free molecules. One can introduce different quantities characterizing adsorption. The excess adsorption isotherm of an individual component is defined as

$$\Gamma^{(k)} = \int(\rho_s^{(k)}(z) - \rho_{sb}^{(k)})dz \quad (12)$$

The total excess adsorption of the fluid is given by

$$\Gamma^{(F)} = \int(\rho_s^{(F)}(z) - \rho_{sb}^{(F)})dz \quad (13)$$

where $\rho_s^{(F)} = \rho_s^{(1)} + \rho_s^{(2)}$ is the total segment density of the fluid and $\rho_{sb}^{(F)}$ is its value in the bulk phase.

Because of the considerable incompressibility of liquids, the excess $\Gamma^{(F)}$ is close to zero. However, molecules of different species can compete for room in the surface layer. Molecules of a given component are displaced by molecules of the other component in the surface region. A composition of the liquid mixture depends considerably on the distance from the wall. To characterize a composition of the mixture of free molecules (components 1 and 2) we introduce the local volume fraction of the kth component in the solution

$$x^{(k)} = \frac{\rho_s^{(k)}(\sigma^{(k)})^3}{\rho_s^{(1)}(\sigma^{(1)})^3 + \rho_s^{(2)}(\sigma^{(2)})^3} k = 1, 2 \quad (14)$$

Notice that $x^{(k)}$ is not the volume fraction in the whole system (where the volume occupied by the grafted chains is also included).

Adsorption from solutions has a strongly competitive character. Therefore, this process is usually characterized by the relative excess adsorption defined as[30,31,67−71]

dx.doi.org/10.1021/jp4027546 | J. Phys. Chem. B XXXX, XXX, XXX−XXX

$$N_k^e = \int dz(x^{(k)}(z) - x_b^{(k)}) \quad (15)$$

where $x_b^{(k)}$ is the volume fraction in the bulk solution. One can easily show that $N_2^e = -N_1^e$. It should be pointed out that the relative excess, N_k^e, can be immediately compared with experimental data.[67−71] The relative excess N_k^e is proportional to the difference in the bulk composition before and after adsorption. In the case of adsorption from a solution of arbitrary composition we cannot estimated the excesses $\Gamma^{(k)}$ from adsorption measurements. For this reason the relative excess adsorption isotherms are commonly used.

In this work the parameter $\varepsilon^{(PP)}$ is used as the unit of energy ($\varepsilon^{(PP)} = \varepsilon \equiv 1$), whereas the diameter of segments of the grafted chains ($\sigma^{(P)} = \sigma \equiv 1$) is the unit of the length. We assume that segments of all components have the same diameters $\sigma^{(k)} = \sigma$ (k = P,1,2). The reduced densities are defined as usual $\rho_s^{(k)}* = \rho_s^{(k)}\sigma^3$, $\rho_s^{(F)}* = \rho_s^{(F)}\sigma^3$, and $\rho_P^* = \rho_P\sigma^2$. The reduced temperature is given by $T^* = k_BT/\varepsilon$. We introduce also the Flory−Huggins type parameters $\chi^{(kl)} = -(\varepsilon^{(kl)} - 0.5(\varepsilon^{(kk)} + \varepsilon^{(ll)}))$. The parameter $\chi^{(Pk)}$ characterizes the quality of the kth solvent with respect to the tethered chains. The parameter $\chi^{(12)}$ describes the nature of the bulk solution.

RESULTS AND DISCUSSION

As has been already mentioned we have considered an interface similar to that existing in a chromatographic system with a chemically bonded phase. We have modeled the surface of a polar substrate (e.g., silica gel) covered by tethered alkyl-like chains. As in the most popular chemically bonded phases the grafted chains were assumed to be short. Such a modified adsorbent was immersed into a liquid mixture consisting of short chains and small spherical molecules.

The free chains (the component 1) could be chemically different from the grafted chains. The similar systems have been studied by Milchev et al.[41] In this way we have modeled heterogeneous molecules, for example, hydrocarbon chains with functional groups. We have assumed that interactions of all segments with the environment are averaged in the molecule. In our model the grafted chains are inert with respect to the substrate because alkanes are rather weakly attracted by the surface of silica gel. However, polar groups in the mobile chains can change their interactions with the substrate. Such molecules are attracted by residual groups OH on the surface of the silica gel.[70] Therefore, we have assumed the Lennard-Jones (9-3) potential to describe these interactions (eq 3).

The monomers (the component 2) can mimic different small molecules, either typical organic solvents (such as, for example, carbon tetrachloride, chloroform, methanol, acetonitrile) or water. These molecules can in a different way interact with the substrate; namely, nonpolar molecules are weakly attracted by the wall, whereas for polar molecules the attraction is strong.

The equilibrium properties of grafted chain layers depend upon numerous parameters. One of the most important is the grafting density. The influence of the grafting density on the height of the grafted chain layer has been intensively studied.[47−49] For very low surface coverages the height is independent of the grafting density. Under these conditions a single grafted chain is isolated, and other chains do not affect its configuration. At sufficiently high grafting densities the tethered chains overlap, and repulsive forces enforce the chains to stretch in a direction perpendicular to the wall. As a consequence, the thickness of the layer increases quickly with increasing grafting density. The dense layer of strongly stretched chains forms the so-called brush.[47] In this region the well-known scaling relation $h^* \sim \rho_P^\gamma$ holds. The exponent γ depends upon the solvent quality[32] and composition.[33] In this paper we deal with moderately dense bonded layers, $\rho_P^* = 0.1$. This value lies in an interval where the height starts to increase rapidly with a rise of the grafting density.[33]

The structure of the surface layer depends upon complex interplay between the grafted chain-grafted chain, grafted chain−fluid and fluid−fluid interactions, as well as interactions of all species with the underlying substrate. In our model the parameters $\varepsilon_s^{(k)}$ and $\varepsilon^{(Pk)}$ characterize interactions of the kth component with the wall and segments of the grafted chains, respectively. The interactions in the liquid mixture are characterized by the parameters: $\varepsilon^{(11)}$ (oligomer−oligomer), $\varepsilon^{(22)}$ (monomer−monomer), and $\varepsilon^{(12)}$ (oligomer−monomer).

To limit the number of parameters of the model we have assumed that $\varepsilon^{(PP)} = \varepsilon^{(P2)} = \varepsilon^{(22)} = 1$ and $\varepsilon_s^{(2)} = 1$. The remaining energy parameters have been varied. The results presented below have been obtained for $M_P = 8$ (Figures 1, 2, and 7−12) and $M_P = 18$ (Figures 3−6). The reduced total segment density of the fluid in the bulk phase, $\rho_{sb}^{(F)}* = \rho_{sb}^{(1)}* + \rho_{sb}^{(2)}*$, was fixed at $\rho_{sb}^{(F)}* = 0.66$. All calculations have been carried out at the temperature $T^* = 3$.

We have analyzed thermodynamic properties of the investigated systems. In this order we calculated the thermodynamic potential $Y = Y(\rho_{sb}^{(1)}, \rho_{sb}^{(2)}, \rho_P)$ for different parameters. Under the assumed conditions the thermodynamic potential was always a smooth function of the system parameters $(\rho_{sb}^{(1)}, \rho_{sb}^{(2)}, \rho_P)$. In the studied cases we have not observed phase transitions. In particular, the mixture of free molecules is within the stable liquid part of the bulk phase diagram.[32] Moreover, the bulk oligomer−monomer mixture does not undergo phase separation. We have not found unstable states for the grafted layers. In general, if a grafted layer is immersed into a poor solvent it can undergo a microphase separation into domains of large local concentration of grafted chain segments and becomes inhomogeneous in the xy-plane. Our theory does not reproduce such transitions. However, the microphase transitions were observed only for grafting densities much lower than those considered in this study.[19]

We have treated the system for which $\varepsilon^{(kl)} = \varepsilon_s^{(k)} = 1$ as a kind of reference system and carried out calculations changing only one parameter with the remaining parameters being fixed. We have studied the influence of the following parameters on the thickness of the bonded layer: (i) length of the free chains (oligomers) (M_1), (ii) interactions of oligomers with segments of the grafted chains ($\varepsilon^{(P1)}$) and with the solid surface ($\varepsilon_s^{(1)}$), and (iii) interactions in the liquid ($\varepsilon^{(11)}$ and $\varepsilon^{(12)}$). The calculations have been performed for different values of the volume fraction of oligomers in the solution ($x_b^{(1)}$).

We start with the discussion of the properties of the grafted layer immersed in a pure solvent consisting of short chains. Figure 1 shows the dependences of the height of the grafted layer on the length of mobile chains. These functions have been calculated for different strengths of grafted chain−oligomer attraction ($\varepsilon^{(P1)}$). One sees that independently of the solvent quality the thickness of the surface layer decreases with increasing length of the mobile chains to a certain limiting value. The mean-field approach[4] and the self-consistent field theory[8,17] lead to analogous conclusions. Notice that the

dx.doi.org/10.1021/jp4027546 | J. Phys. Chem. B XXXX, XXX, XXX−XXX

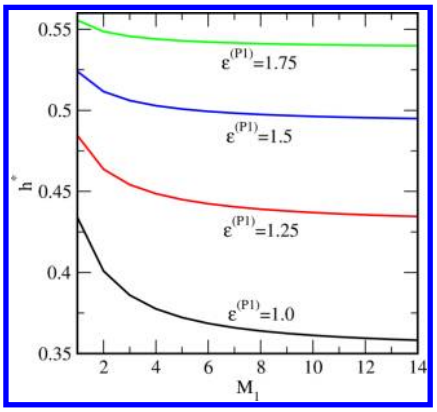

Figure 1. Normalized height of the grafted chain layer in contact with a pure solvent as a function of the mobile chain length for different values of the parameter characterizing grafted chain−solvent interactions $\varepsilon^{(P1)}$ = 1.0 (black line), 1.25 (red line), 1.5 (blue line), and 1.75 (green line). The remaining energy parameters are $\varepsilon_s^{(1)} = \varepsilon^{(11)} = \varepsilon_s^{(k)}$ = 1.0. The length of the grafted chains is M_P = 8.

solvent size effects become negligible when the mobile molecules are longer than the grafted chains ($M_1 > M_P$). Similar theoretical results have been obtained for adsorption from solutions on the chemically bonded phases.[31] Changes in the behavior of chain molecules on chemically bonded phases were also observed in liquid chromatography. This technique is often used to separate solutes that belong to the same homologous series. The solute retention increases with the increasing solute size. The experiments have shown that the increase of retention is much weaker for mobile molecules longer than the bonded chains.[72] To explain the relationships presented in Figure 1 we have analyzed the density profiles of grafted and free chains calculated for different lengths of mobile chains (Figure 2) and for different values of the parameter $\varepsilon^{(P1)}$ (Figure 4).

In Figure 2 we present the segment density profiles of mobile (part a) and of grafted (part b) chains for $\varepsilon^{(P1)}$ = 1 and different M_1. In this case the interactions between all components are the same. The structure of the bonded layer is considerably influenced by the presence of fluid molecules. The grafted and mobile chains compete for room in the surface layer, and the grafted chains are pushed from this region by adsorbing fluid. Short chains quite strongly penetrate the bonded phase and adsorb at the wall. The densities of dimers, trimers, and tetramers near the solid surface are even greater than the density of the bulk liquid. In the remaining part of the surface layer the density of all the mobile chains is always lower than their density in the bulk phase. Longer chains are not able to penetrate the interior of the surface layer. The density of longer free chains is lower near the wall and greater in the outer part of the grafted chain layer. The opposite effects are observed for corresponding density profiles of grafted chains. The segment density of grafted chains near the wall is lower for shorter mobile chains. In the center of the surface layer its density is essentially independent of solvent size. In the outer part of the bonded phase an increase of the oligomer length causes a slight increase of the segment density of tethered chains.

The driving force behind collapse of the grafted chain layer, as the length of the mobile chains increases, is the configurational distortion of the mobile chains in the anisotropic environment of the grafted chains. Within the bonded phase the free chains are stretched into unfavorable

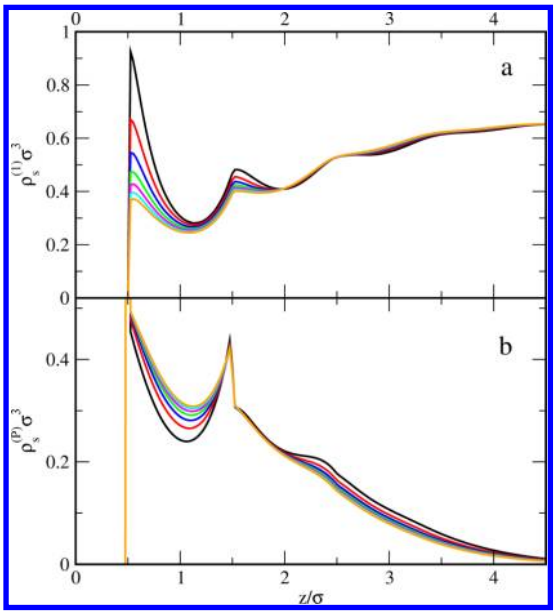

Figure 2. Segment density profiles of mobile (part a) and grafted (part b) chains in a pure solvent for different lengths of three free chains, M_1: 2 (black line), 4 (red line), 6 (blue line), 8 (green line), 10 (magenta line), 12 (cyan line), and 14 (orange line). All energy parameters are identical: $\varepsilon^{(P1)} = \varepsilon^{(11)} = \varepsilon_s^{(1)}$ = 1.0. The length of the grafted chains is M_P = 8.

configurations. Spherical molecules can substantially penetrate the bonded phase and stretch the grafted chains to minimize excluded volume interactions. By contrast, longer mobile chains are expelled from the surface layer, so the bonded layer shrinks. The effects of configurational entropy become more important for long mobile chains. However, when $M_1 > M_P$, only a part of a mobile chain can be stalled in the bonded phase. The remaining part of the mobile chain can almost freely change its configuration. For this reason, the height of the grafted chain layer becomes independent of the length of mobile chains.

Adsorption of free chains is strongly coupled to the solvent quality. This is demonstrated in Figure 3, where the influence of grafted chain−oligomer interactions on the structure of the surface layer is considered. When the strength of grafted chain−

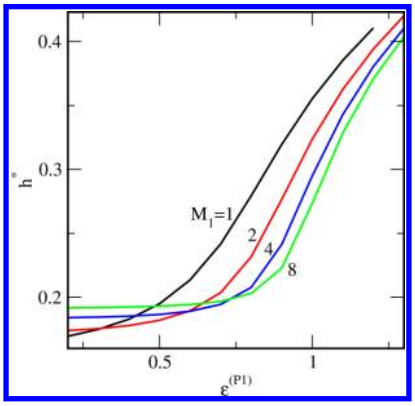

Figure 3. Normalized height of the grafted chain layer in a pure solvent as a function of the parameter characterizing grafted chain−solvent interactions for different lengths of mobile chains: M_1 = 1 (black line), M_1 = 2 (red line), M_1 = 4 (blue line), and M_1 = 8 (green line) The remaining energy parameters are $\varepsilon^{(P1)} = \varepsilon^{(11)} = \varepsilon_s^{(1)}$ = 1.0. The length of grafted chains is M_P = 18.

dx.doi.org/10.1021/jp4027546 | J. Phys. Chem. B XXXX, XXX, XXX−XXX

oligomer attraction ($\varepsilon^{(P1)}$) increases the bonded chains become more and more stretched. The shape of the curve h^* vs $\varepsilon^{(P1)}$ depends on the length of the mobile chains. For small fluid molecules the normalized height gradually increases with an increase of the parameter $\varepsilon^{(P1)}$. However, for tetramers and octamers the height remains almost constant at low values of $\varepsilon^{(P1)}$ and increases rapidly for $\varepsilon^{(P1)} > 1$. In the case of good solvents (high $\varepsilon^{(P1)}$) an increase of the length of mobile chains leads to a decrease of the height of the bonded layer. For bad solvents (low $\varepsilon^{(P1)}$) an inverse effect is found. As was mentioned earlier, the compatibility of the mobile and grafted chains can also be described in terms of Flory–Huggins parameter $\chi^{(P1)}$. Under assumed conditions the parameter $\chi^{(P1)}$ decreases as $\varepsilon^{(P1)}$ increases.

In Figure 4 we present examples of density profiles of mobile tetramers (part a) and grafted 18-mers (part b) for selected

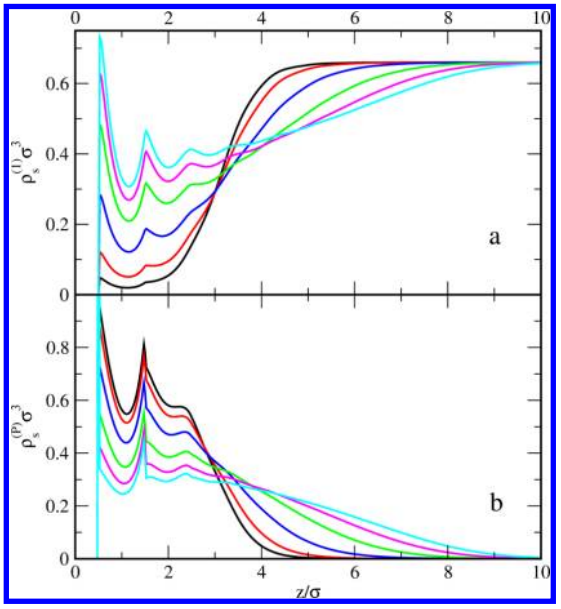

Figure 4. Segment density profiles of mobile (part a) and grafted (part b) chains in a pure solvent consisting of tetramers ($M_1 = 4$) for different values of the parameter characterizing grafted chain–solvent interactions $\varepsilon^{(P1)} = 0.7$ (black line), 0.8 (red line), 0.9 (blue line), 1.0 (green line), 1.1 (magenta line), and 1.2 (cyan line). The remaining energy parameters are $\varepsilon^{(11)} = \varepsilon_s^{(1)} = 1.0$. The length of the grafted chains $M_P = 18$.

values of the parameter $\varepsilon^{(P1)}$. When grafted chain–tetramer attraction becomes stronger the density of tetramers in the interior of the bonded phase considerably increases and decreases in the outer region. An intersection occurs between the profiles in the central part of the bonded phase. The opposite effects are visible for density profiles of grafted chains. The general trend is the following: more adsorbed molecules - less segments of tethered chains. Accumulation of fluid molecules near the wall causes segments of the grafted chains to be pushed off the wall. The height of the bonded layer gets larger. However, when grafted chain–tetramer contacts are energetically unprofitable, the density of tetramers in the vicinity of the surface is very low. Then, the segments of grafted chains are able to"condensate" into a thin film on the wall (see the structure of the bonded phase for $\varepsilon^{(P1)} = 0.7$).

Figure 5a illustrates the impact of the solid–fluid interactions on the thickness of the surface layer for selected oligomers. The

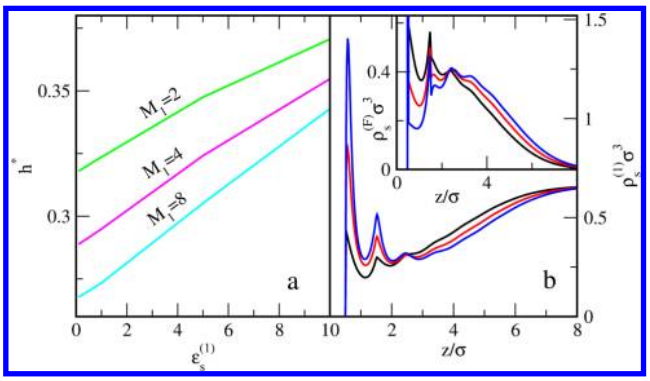

Figure 5. (part a) Normalized height of the grafted chain layer for a pure solvent as a function of the parameter characterizing the solvent–substrate interactions for three lengths of mobile chains: $M_1 = 2$ (green line), $M_1 = 4$ (magenta line), and $M_1 = 8$ (cyan line). (part b) Segment density profiles of mobile chains in a pure solvent consisting of tetramers ($M_1 = 4$) for different values of the parameter characterizing the solvent–substrate interactions $\varepsilon_s^{(1)}$: 0.1 (black line), 5 (red line), and 10 (blue line). In the inset the corresponding segment density profiles of grafted chains are shown. The remaining energy parameters are $\varepsilon^{(P1)} = \varepsilon^{(11)} = \varepsilon_s^{(1)} = 1.0$. The length of the grafted chains is $M_P = 18$.

substrate attracts fluid molecules, so the mobile chains accumulate close to the surface. The presence of fluid molecules near the wall leads to stretching. As an example, we show the density profiles of mobile tetramers and of grafted chains for different adsorption energies of oligomer segments, $\varepsilon_s^{(1)}$ (see Figure 5b), of the grafted chains. Obviously, greater adsorption energy causes stronger expansion of the bonded phase. Notice that under the assumed conditions the height is a linear function of the parameter $\varepsilon_s^{(1)}$.

Next, we discuss the influence of oligomer–oligomer interactions ($\varepsilon^{(11)}$) on the structural rearrangement of the grafted chains in a pure solvent (see Figure 6). We present here the results obtained for mobile monomers, dimers, tetramers,

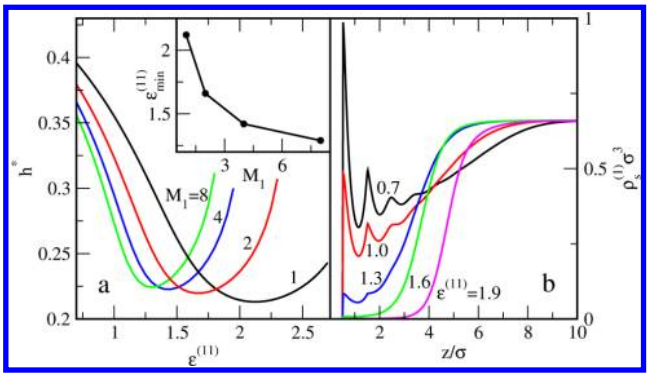

Figure 6. (part a) Normalized height of the grafted chain layer in a pure solvent as a function of the parameter characterizing the solvent–solvent interactions for four lengths of mobile chains: $M_1 = 1$ (black line), $M_1 = 2$ (red line), $M_1 = 4$ (blue line), and $M_1 = 8$ (green line). In the inset the minimal energy $\varepsilon_{min}^{(P1)}$ is plotted as a function of solvent size (M_1). (part b) Segment density profiles of mobile chains in a pure solvent consisting of tetramers ($M_1 = 4$) for different values of the parameter characterizing the solvent–solvent interactions $\varepsilon^{(11)}$: 0.7 (black line), 1.0 (red line), 1.3 (blue line), 1.6 (green line), and 1.9 (magenta line). In the inset the corresponding segment density profiles of grafted chains are shown. The remaining energy parameters are $\varepsilon^{(P1)} = \varepsilon_s^{(1)} = 1.0$. The length of the grafted chains is $M_P = 18$.

dx.doi.org/10.1021/jp4027546 | J. Phys. Chem. B XXXX, XXX, XXX–XXX

and octamers. With an increase of the parameter $\varepsilon^{(11)}$ the height decreases to a minimal value. A further increase of $\varepsilon^{(11)}$ gives a rapid increase of the bonded layer thickness. This can be explained as follows. For low $\varepsilon^{(11)}$ the interactions in the bulk liquid are weaker than the interactions of free chains with the grafted chain segments and with the substrate. Therefore, the mobile chains penetrate the bonded phase and cause its swelling. Inversely, for high $\varepsilon^{(11)}$ the interactions in the bulk phase are stronger than in the surface layer, and the mobile chains are "sucked" from the surface layer, making more room for grafted chains that can expand. Additionally, the fluid molecules located on the top of the bonded layer attract the grafted chains in the direction of the bulk phase. At the minimum of $h^*(\varepsilon^{(11)})$ both effects are compensated.

The height decreases with increasing M_1 at low values of $\varepsilon^{(11)}$, whereas it increases for strong oligomer−oligomer attraction. The parabolic curve h^* vs $\varepsilon^{(11)}$ becomes narrower for longer mobile chains. It is worth pointing out that the minimum on the dependence of h^* vs $\varepsilon^{(11)}$ shifts to lower values of $\varepsilon^{(11)}$ for longer mobile chains (see the inset in Figure 6a). A tendency to form clusters in the bulk phase is stronger for longer chains. Therefore, the effect of "sucking" longer chains from the surface layer occurs for weaker segment−segment attraction in the fluid. The above conclusions can be confirmed by the analysis of the selected density profiles.

In Figure 6b we have drawn the density profiles of mobile tetramers for several values of the parameter $\varepsilon^{(11)}$. We see that, except for accumulation of tetramers at the wall for $\varepsilon^{(11)} = 0.7$, the tetramer densities within the bonded layer are significantly lower than the bulk density. The distribution of fluid molecules in the surface layer depends considerably on the strength of tetramer−tetramer interactions. One can distinguish here two types of distributions, namely, the profiles with oscillations near the wall and the continuous, step-like profiles. For $\varepsilon^{(11)} = 0.7$ ($\chi^{(P1)} = -0.15$) we have three peaks close to the surface and a long tail, where the density slowly increases to the bulk value. When tetramer−tetramer interactions are highly favorable ($\varepsilon^{(11)} = 1.9$; $\chi^{(P1)} = 0.45$) the step-like profile is found. The tetramers are practically absent in the interior of the bonded layer. Their density increases rapidly at $z^* \approx 4$ and quickly achieves the bulk value, $\rho_{sb}^{(1)}$. Close to the substrate the density $\rho_s^{(1)}(z)$ always decreases with increasing $\varepsilon^{(11)}$. The picture is more complicated in the outer part of the surface layer. In this region the considered profiles intersect. Notice that the distance, z', where the density attains the bulk value, $\rho_s^{(1)}(z') = \rho_s^{(1)}$, changes as $\varepsilon^{(11)}$ rises. Initially, this distance decreases ($z'(\varepsilon^{(11)} = 0.7) = 10.23$, $z'(\varepsilon^{(11)} = 1.0) = 9.23$, and $z'(\varepsilon^{(11)} = 1.3) = 7.55$), whereas for high values of $\varepsilon^{(11)}$ this sequence inverses ($z'(\varepsilon^{(11)} = 1.6) = 7.50$ and $z'(\varepsilon^{(11)} = 1.9) = 9.18$). The change corresponds to the minimum on the curve h^* vs $\varepsilon^{(11)}$, $\varepsilon_{min}^{(11)} = 1.42$.

For weak tetramer−tetramer interactions the structure of the bonded layer is dominated by the excluded volume effects. The segments of grafted chains are pushed from the surface layer by the adsorbed molecules. This effect diminishes as the tetramer penetration weakens and the bonded phase shrinks. For sufficiently strong tetramer−tetramer interactions the mechanism of surface layer expansion is different. We see now that tetramers are not able to penetrate the grafted chain layer. However, they adsorb "on the bonded phase". The grafted chains become unperturbed by fluid molecule configurations and expand in the direction perpendicular to the surface. This effect is altered by attraction between adsorbed tetramers and end segments of grafted chains

Let us consider now the behavior of the grafted chain layer in contact with oligomer−monomer solution. The bonded phase is selectively permeable to free molecules of different sizes. Local changes in densities of the mixture components have important consequences for the structure of the surface layer. Figure 7 shows the dependences of the height on the mixture composition for different oligomers and four values of the parameter $\varepsilon^{(P1)} = 1.0$, 1.25, 1.5, and 1.75. The remaining energy parameters are fixed $\varepsilon^{(kl)} = \varepsilon_s^{(1)} = 1$. In part a we present the results obtained for all the energy parameters having the same value ($\varepsilon^{(P1)} = 1$). Then Flory−Huggins parameters, $\chi^{(kl)}$, for all pairs of species in the system are equal to zero. In this case the height decreases monotonically with an increase of oligomer concentration. Moreover, at a given mixture composition, the thickness of the surface layer is lower for longer oligomers. Similarly, as in pure solvents this effect diminishes for sufficiently long mobile chains.

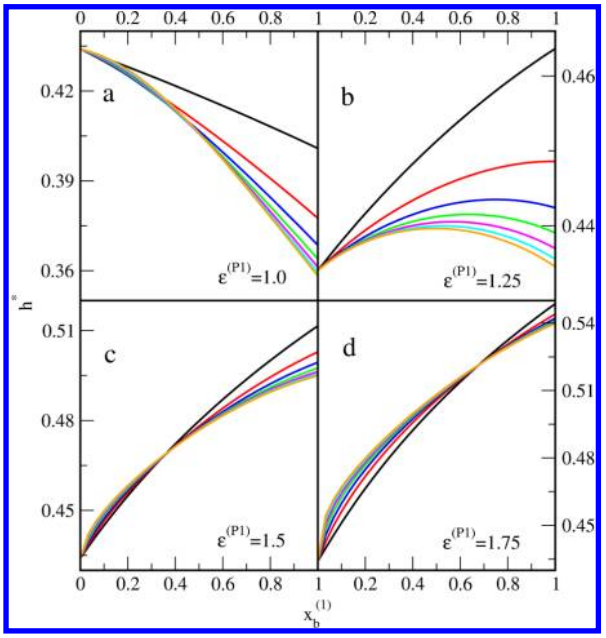

Figure 7. Normalized height of the grafted chain layer in the oligomer−monomer mixture as a function of its composition for different parameters characterizing grafted chain−oligomer interactions $\varepsilon^{(P1)}$: 1.0 (a), 1.25 (b), 1.5 (c), and 1.75 (d) and for different oligomer lengths: $M_1 = 2$ (black line), $M_1 = 4$ (red line), $M_1 = 6$ (blue line), $M_1 = 8$ (green line), $M_1 = 10$ (magenta line), $M_1 = 12$ (cyan line), and $M_1 = 14$ (orange line). The remaining energy parameters are $\varepsilon^{(P2)} = \varepsilon^{(kl)} = \varepsilon_s^{(k)} = 1.0$; $k,l = 1, 2$. The length of the grafted chains is $M_P = 8$.

A qualitative change is observed for energetically profitable grafted chain−oligomer interactions (see Figure 7b−7d). In this case, there are two opposite effects in determining the height. On the one hand, attractive grafted chain−oligomer interactions cause penetration of mobile chains into the bonded phase. This, in turn, contributes to the expansion of the grafted chains. On the other hand, the presence of free chains in the bonded phase is still disfavored because of the loss of their configurational entropy. Therefore, the mobile chains exhibit the tendency to remove the surface layer. The equilibrium depends also on the mixing entropy in the liquid mixture. The interplay between these factors leads to interesting results.

dx.doi.org/10.1021/jp4027546 | J. Phys. Chem. B XXXX, XXX, XXX−XXX

When the affinity of oligomers to grafted chains is relatively weak ($\varepsilon^{(P1)}$ = 1.25) the shape of the curve h^* vs $x_1^{(1)}$ depends on the oligomer length. For short mobile chains (M_1 = 2, 3, 4) h^* is an increasing function in the whole concentration region. For longer oligomers a maximum on the curve h^* vs $x_b^{(1)}$ appears. This maximum shifts to lower oligomer concentrations as its length increases. One can conclude that for sufficiently high concentrations of longer oligomers the entropic effects prevail over enthalpic interactions, and the height decreases as in the previous case.

If grafted chain−oligomer attractive interactions are much stronger ($\varepsilon^{(P1)}$ = 1.5 and 1.75) the height always increases as the oligomer concentration increases. The increase of the thickness of the bonded layer with increasing concentration of the better solvent has been observed in experiments[73] and in molecular simulations.[36,44,45] Now, the enthalpic effects dominate in the entire concentration range. The curves h^* vs $x_b^{(1)}$ plotted for different oligomers cross over one another. An interesting behavior is observed for dilute solutions, where the thickness of the grafted layer slightly increases with increasing oligomer length. When $x_b^{(1)} \to 1$ the effect is the same as in the pure oligomeric fluid.

To highlight the mechanism of the surface layer expansion with varying composition of the solution we have analyzed selected density profiles of mobile chains and the total density profiles of adsorbed fluid.

In Figure 8 we show the segment density profiles of several oligomers for $\varepsilon^{(P1)}$ = 1. The oligomer density within the

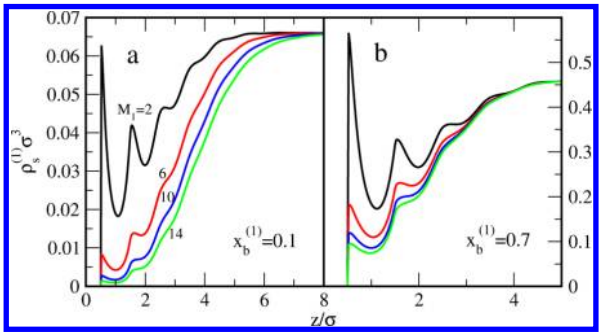

Figure 8. Segment density profiles of mobile chains in oligomer−monomer mixtures for two values of the volume fraction $x_1^{(1)}$ = 0.1 (part a) and 0.7 (part b) and for different oligomer lengths M_1 = 2 (black line), 6 (red line), 10 (blue line), and 14 (green line). The parameter characterizing grafted chain−oligomer interactions is equal to $\varepsilon^{(P1)}$ = 1.0. The remaining energy parameters are: $\varepsilon^{(P2)} = \varepsilon^{(kl)} = \varepsilon_s^{(k)}$ = 1.0; k,l = 1,2. The length of the grafted chains is M_P = 8.

bonded phase is significantly lower than in the bulk liquid (except for the dimer density at the wall for $x_b^{(1)}$ = 0.7). Depletion in the oligomer density is deeper for longer mobile chains in the whole concentration region. The structure of the surface layer is dictated mainly by entropy effects. The oligomers penetrate the bonded phase much weaker than the monomers. As the result, an increase of oligomer concentration leads to the shrinkage of the grafted chain layer (see Figure 7a).

Figure 9 shows the density profiles of oligomers calculated for preferential grafted chain−oligomer interactions ($\varepsilon^{(P1)}$ = 1.5). Now, the influence of grafted chain−oligomer interactions is especially important for dilute solutions. In contrast to the situation shown in Figure 8a, the oligomer density in the surface layer is greater than the bulk value $\rho_{sb}^{(1)}$. An increase of the oligomer length causes a slight decrease of the oligomer

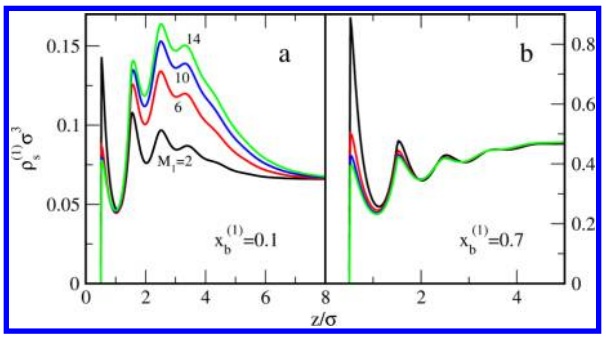

Figure 9. Same as in Figure 8 but for favorable grafted chain−oligomer interactions. The parameter characterizing the grafted chain−oligomer interactions is equal to $\varepsilon^{(P1)}$ = 1.5.

density in an immediate vicinity of the wall and a considerable increase in the remaining part of the bonded phase. However, for greater content of oligomers in the bulk liquid, the density of longer oligomers is lower within the whole surface layer. Nevertheless, the oligomers are able to penetrate the bonded phase to a considerable degree. This results in the stretching of the grafted chains. (see Figure 7c).

Figure 10 depicts the total segment density of the fluid, $\rho^{(F)}$, for several volume fractions of tetramers in the bulk monomer−

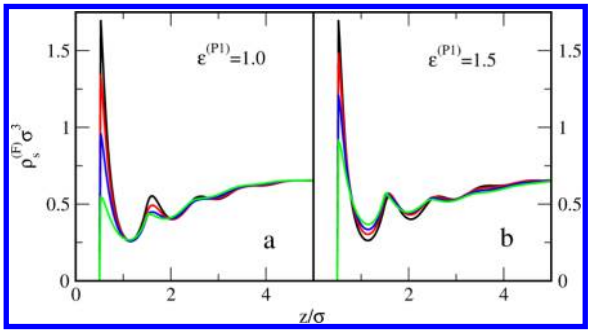

Figure 10. Total segment density profiles of the tetramer−monomer mixture, $\rho_s^{(F)} = \rho_s^{(1)} + \rho_s^{(2)}$, for two values of the energy parameters $\varepsilon^{(P1)}$, 1.0 (part a) and 1.5 (part b), and for different values of the volume fraction of tetramer in the bulk phase $x_b^{(1)}$ = 0 (black line), 0.33 (red line), 0.66 (blue line), and 1.0 (green line). The remaining energy parameters are $\varepsilon^{(P2)} = \varepsilon^{(kl)} = \varepsilon_s^{(k)}$ = 1.0; k,l = 1,2. The length of the grafted chains is M_P = 8.

tetramer solution. As previously, we have carried out calculations for two values of the parameter $\varepsilon^{(P1)}$ = 1.0 (part a) and $\varepsilon^{(P1)}$ = 1.5 (part b). For $\varepsilon^{(P1)}$ = 1.0 an increase of tetramer concentration generates a decrease of the total fluid density in the interior of the bonded phase (up to $z \approx 2.5$) and causes an inverse effect in the outer part of the surface layer. A lower fluid density inside the bonded phase results in a weaker swelling of the grafted chains. Therefore, the height of the bonded layer is a decreasing function of the volume fraction $x_b^{(1)}$ (see Figure 7a). For stronger grafted chain−tetramer interactions ($\varepsilon^{(P1)}$ = 1.5) an increase of $x_b^{(1)}$ causes an increase of the total fluid density only at the wall and on top of the bonded layer, but the opposite result is observed in a wide region within the bonded phase center. As a consequence, the grafted chains are pushed by the fluid molecules, so the height increases (see Figure 7c). Notice that the influence of the mixture composition on the total fluid density is rather weak. By contrast, the density profiles of oligomers depend considerably on the volume fraction $x_b^{(1)}$ (cf. parts a and b in

dx.doi.org/10.1021/jp4027546 | J. Phys. Chem. B XXXX, XXX, XXX−XXX

Figures 8 and 9). A composition of the fluid in the bonded phase results from a competitive adsorption of oligomers and monomers. The height of the grafted chain layer is dictated mainly by the concentration of oligomers in the surface region.

Now, we would like to show how molecular interactions in the bulk liquid can affect the structure of the grafted layer. The effects connected with the change of the strength of oligomer–oligomer interactions are shown in Figure 11a. When the

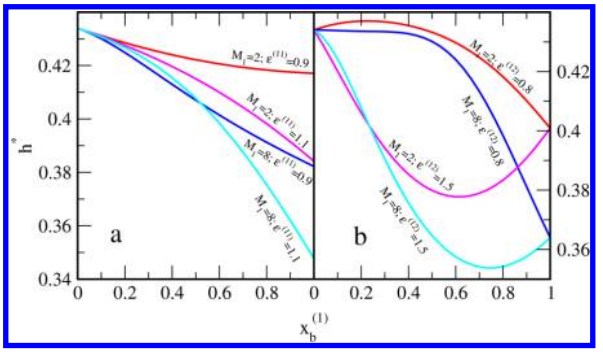

Figure 11. Effects of the oligomer–oligomer (part a) and oligomer–monomer interactions (part b) on the normalized height of grafted chains immersed in the oligomer–monomer mixture. (part a) Normalized height of the grafted chain layer for dimers (M_1 = 2) and two values of $\varepsilon^{(11)}$ = 0.9 (red line) and 1.1 (magenta line) and for octamers (M_1 = 8) and two values of $\varepsilon^{(11)}$ = 0.9 (blue line) and 1.1 (cyan line); $\varepsilon^{(12)}$ = 1.0. (part b) Normalized height of the grafted chain layer for dimers (M_1 = 2) and for two values of $\varepsilon^{(12)}$ = 0.8 (red line) and 1.5 (magenta lie) and for octamers (M_1 = 8) and two values of $\varepsilon^{(11)}$ = 0.8 (blue line) and 1.5 (cyan line); $\varepsilon^{(11)}$ = 1.0. The remaining energy parameters are $\varepsilon^{(Pk)} = \varepsilon_s^{(k)}$ = 1.0; k,l = 1,2. The length of the grafted chains is M_P = 8.

parameter $\varepsilon^{(11)}$ increases, the bonded chains immersed in the dimer–monomer solution are always compressed because dimers are "sucked" from the surface layer by the dimers in the bulk liquid. The same relations are observed for high concentrations of octamers. However, in the dilute solutions an increase of octamer–octamer attraction causes a rise of the bonded phase thickness. Figure 11b illustrates the impact of oligomer–monomer interactions on the shape of the curve h^* vs $x_b^{(1)}$. In the case of energetically profitable oligomer–monomer contacts a deep minimum on the curve $h^*(x_b^{(1)})$ appears. When these interactions are weaker a small maximum is observed for dimers, while for octamers the height is a decreasing function of the volume fraction, $x_b^{(1)}$. These examples indicate that the influence of molecular interactions in the liquid can strongly affect the structure of the grafted layer.

The above discussion has shown that the curves h^* vs $x_b^{(1)}$ have different shapes depending on the relation between the parameters characterizing the system. In particular, a maximum or a minimum can occur for a certain composition of the liquid mixture. This finding is interesting for potential practical applications of the bonded phases.

We have already noticed that the thickness of the grafted layer depends on adsorption of different components on the surface modified with grafted chains. The height of the tethered chain layer is correlated with the relative excess adsorption of a given component.[33] The evolution of the relative excess adsorption isotherms from oligomer–monomer solutions with increasing parameter $\varepsilon^{(P1)}$ has been discussed in our previous paper.[31] When all energy parameters are the same (as in Figure 7a), the relative excess adsorption of oligomers is always negative and decreases for longer chains (see Figure 1a in ref 31). In other words, the average concentration of oligomers in the surface layer is smaller than the concentration in the bulk solution. On the contrary, the enhancement of the monomer concentration in the surface phase is observed. The situation changes when grafted chain–oligomer attraction becomes sufficiently strong. For $\varepsilon^{(P1)}$ = 1.5 (as in Figure 7c) all considered oligomers are always preferentially adsorbed in the bonded phase (see Figure 1c in ref 31).

To illustrate the connection between the height of the grafted chain layer and adsorption we discuss here the system for which $\varepsilon^{(P1)}$ = 1.4. Figure 12 presents the curves h^* vs $x_b^{(1)}$

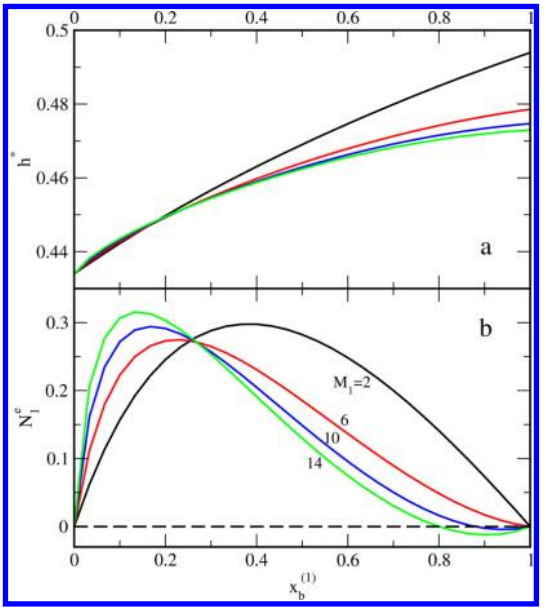

Figure 12. (part a) Normalized height of the grafted chain layer in an oligomer–monomer mixture as a function of its composition for $\varepsilon^{(P1)}$ = 1.4 and for different oligomer lengths M_1 = 2 (black line), M_1 = 6 (red line), M_1 = 10 (blue line), and M_1 = 14 (green line). (part b) Relative excess adsorption isotherms of the oligomers from part a. The remaining energy parameters are $\varepsilon^{(P2)} = \varepsilon^{(kl)} = \varepsilon_s^{(k)}$ = 1.0; k,l = 1,2. The length of the grafted chains is M_P = 8.

(part a) and the relative excess adsorption isotherms N_1^e vs $x_b^{(1)}$ (part b) for several oligomers. In this case the height is an increasing function of the volume fraction of oligomers in the bulk phase. It is worth mentioning that the curves h^* vs $x_b^{(1)}$ and the relative excess adsorption isotherm plotted for different lengths of mobile chains intersect in the same concentration region $0.17 < x_b^{(1)} < 0.26$. For dilute solutions, the adsorption of oligomers and the height increase as M_1 increases. However, for high volume fractions $x_b^{(1)}$ we see lowering of the oligomer adsorption and the height of the bonded layer for longer mobile chains. The relative excess adsorption of dimers and tetramers is positive in the whole concentration region. When mobile chains are longer, the adsorption azeotropy is found. There exists such a mixture composition, for which the average compositions of the mixture in the bonded phase and in the bulk solution are the same. At the azeotropic point the relative excesses of both components are equal to zero, $N_1^e(x_{az}^{(1)}) = N_2^e(x_{az}^{(1)}) = 0$. The azeotropic point shifts to unity for shorter oligomers.

dx.doi.org/10.1021/jp4027546 | J. Phys. Chem. B XXXX, XXX, XXX–XXX

Adsorption of oligomers results from a balance between the entropic expulsion from the surface layer, the attractive forces extorted by the wall and by the grafted chains, and interactions in the bulk phase. The reduction in conformational entropy in the interphase region is greater for longer oligomers. For short mobile chains attractive interactions dominate. The mechanism of the process is similar for dilute solutions of longer chains. Then, the entropic effects prevail, and adsorption of oligomers becomes less profitable. The grafted chains change their conformations to minimize the free energy of the system.

CONCLUSIONS

In this paper we have studied the structure of the grafted chain layer immersed in an explicit solvent consisting of chain molecules. We have used the density functional theory for modeling the bonded layer behavior in response to changes in its environment. We have assumed that the substrate does not attract grafted chains. However, the fluid molecules interact with the surface via Lennard-Jones (9-3) potential. The interactions between the mobile chains, monomers, as well as segments of tethered chains are described by Lennard-Jones (12-6) potential. We have studied the layers built of short grafted chains, at the moderate grafting density. We have investigated the grafted chain layers in contact with oligomeric solvents and oligomer−monomer solutions.

We have attempted to resolve a few of the lingering questions about the layers of tethered chains. First, we have dealt with the bonded layers immersed in one-component solvents. The impact of selected parameters on the structure of the surface layer has been systematically analyzed. We have shown that the height of the grafted chain layer decreased to a certain limiting value as the size of the solvent molecules increased. When mobile chains become longer than the grafted chains, the thickness of the bonded phase is almost constant. We have also examined the influence of the grafted chain−fluid interactions on the structure of the bonded layer. As one can expect, the height rises noticeably with the strength of the grafted chain−fluid attraction. Variation of the fluid−fluid interactions leads to more interesting effects. When interactions between fluid molecules are much more energetically profitable than grafted chain−fluid and fluid−substrate interactions, the height of the bonded layer increases. Conversely, for unprofitable fluid−fluid interactions an increase of their strength causes shrinking of the bonded layer.

We have inspected segment density profiles of the grafted and mobile chains in various systems. We have concluded that the investigated oligomers are able to penetrate the bonded phase to a considerable degree. The surface layer is highly inhomogeneous. The density profiles of both grafted and mobile chains are correlated. In general, an increase of the fluid density in the surface layer causes the grafted chain layer to be more extended. Despite that the assumptions underlying the model differ from those involved in other papers, our conclusions are consistent with the predictions of the self-consistent field theory.[4,8,17]

Next, we have examined the behavior of grafted chains in oligomer−monomer solutions. We have focused on the problem how the solvent composition affects the bonded layer thickness. We have analyzed the height of tethered chain layers as a function of the oligomer concentration in the bulk mixture, h^* vs $x_1^{(1)}$. The shape of such a curve depends strongly on the relations between parameters characterizing the system. The thickness of the bonded phase can be either an increasing or decreasing function of the oligomer volume fraction. For certain values of the energy parameters and oligomer lengths this function can possess a minimum or a maximum. When all energy parameters are the same, an increase of the oligomer content in the bulk phase always causes the compression of the bonded layer. However, for profitable grafted chain−oligomer interactions the opposite effects are observed. These findings are consistent with experiments[61,73] and with computer simulations.[36,44,45] We have also signaled that the interaction in the bulk solution can considerably affect the structure of the grafted chain layers. The changes in the thickness of the bonded layer with a change of solvent composition were continuous. In the considered thermodynamic conditions we have not found phase transitions in the grafted chain layer. It is consistent with the experimental results of Doye et al.[61] who investigated the structure of C_{18}-bonded stationary phases in various mixed solvents and did not find the phase collapse upon changing the bulk phase composition from an organic solvent to an aqueous content.

The analysis of the density profiles of all components leads to the conclusion that the height of the tethered chain layer depends mainly on the composition of the mixture inside the bonded phase. This results from competitive adsorption from the solution on such a "soft adsorbent". We have found that the relative excess adsorption of oligomers is correlated with the height: lower relative excess adsorption of oligomers - a more compressed bonded phase.

The equilibrium in the bonded phase/solution interface results from a very complicated balance between entropic and enthalpic effects, either in the surface layer or in the bulk liquid. Therefore, it is difficult to predict the structure of a bonded layer in a concrete oligomer−monomer solution. In this study we have focused on the qualitative behavior of the grafted chain layers instead of quantitative reproduction of simulation or experimental results by fitting the model parameters. Nevertheless, our conclusions are consistent with some experiments and the results of other theoretical investigations.

It is evident from the above discussion that a change of mixture composition allows us to model the structure of the surface layer. The knowledge of the dependence of the bonded layer height on the mixture composition is important for numerous practical applications. As a prominent example, one can mention chromatography. The structure of the chemically bonded phase is a significant parameter determining retention in liquid chromatography with a mixed mobile phase. In gradient elution chromatography a mobile phase composition is varied to optimize the separation.

The density functional theory captures the fundamental features of the phenomena occurring on the interface, chemically bonded phase/mixed solvent, and may be an effective tool for further investigations.

AUTHOR INFORMATION

Corresponding Author

*E-mail: tstaszew@gmail.com.

Notes

The authors declare no competing financial interest.

ACKNOWLEDGMENTS

This work was partially supported by EC under Grant No. PIRSES-GA2010-268498 (MB).

REFERENCES

(1) Alexander, S. *J. Phys. (France)* **1977**, *38*, 983−987.
(2) de Gennes, P. G. *Macromolecules* **1980**, *13*, 1069−1075.
(3) Lai, P. -Y; Halperin, A. *Macromolecules* **1992**, *25*, 6693−6695.
(4) van Zaten, J. H. *Macromolecules* **1980**, *27*, 5052−5059.
(5) Milner, S. T.; Witten, T. A.; Cates, M. E. *Macromolecules* **1988**, *21*, 2610−2619.
(6) Milner, S. T. *Science* **1991**, *251*, 905−914.
(7) Zhulina, E. B.; Borisov, O. V.; Priamytsin, V. A. *J. Colloid Interface Sci.* **1990**, *137*, 495−511.
(8) Zhulina, E. B.; Borisov, O. V.; Brombacher, L. *Macromolecules* **1991**, *24*, 4679−4690.
(9) Amoskov, V. M.; Birshtein, T. M.; Mercurieva, A. A. *Macromol. Theory Simul.* **2006**, *15*, 46−69.
(10) Fleer, G. J.; Cohen Stuart, M. A.; Scheutjens, J. M. H. M.; Cosgrove, T.; Vincent, B. *Polymers at Interfaces*; Chapman and Hall: London, 1993.
(11) Cosgrove, T.; Heath, T. G.; van Lent, B.; Scheutjens, J. M. H. M.; Leermakers, F. *Macromolecules* **1987**, *20*, 1692−1696.
(12) Leermakers, F. A. M.; Scheutjens, J. M. H. M. *J. Chem. Phys.* **1988**, *89*, 3264.
(13) Scheutjens, J. M. H. M.; Fleer, G. J.; Cohen Stuart, M. A *Colloids Surf.* **1986**, *21*, 285.
(14) Wijmans, C. M.; Scheutjens, J. M. H. M.; Zhulina, E. B. *Macromolecules* **1992**, *25*, 265.
(15) Boehmer, M. R.; Koopal, L. K.; Tijssen, R. *J. Phys. Chem.* **1991**, *95*, 6285−6297.
(16) Steels, B. M.; Koska, J.; Haynes, C. A. *J. Chromatogr. B* **2000**, *743*, 41−56.
(17) Martin, J. I.; Wang, Z. G. *J. Phys. Chem.* **1995**, *99*, 2833−2844.
(18) Netz, R. N; Schick, M. *Macromolecules* **1998**, *31*, 5105−5122.
(19) Carignano, M. A.; Szleifer, I. *J. Chem. Phys.* **1994**, *100*, 3210−3223.
(20) Carignano, M. A.; Szleifer, I. *Macromolecules* **1995**, *28*, 3197−3204.
(21) Carignano, M. A.; Szleifer, I. *J. Chem. Phys.* **1995**, *102*, 8662−8669.
(22) Szleifer, I.; Carignano, M. A. *Adv. Chem. Phys.* **1996**, *94*, 165−260.
(23) McCoy, J. D.; Teixeira, M. A.; Curro, J. G. J. *J. Chem. Phys.* **2002**, *117*, 2975−2986.
(24) Cao, D. P.; Wu, J. *Langmuir* **2006**, *22*, 2712−2718.
(25) Xu, X. F.; Cao, D. P. *J. Chem. Phys.* **2009**, *130*, 164901.
(26) Xu, X.; Cao, D. P. *Soft Matter* **2010**, *6*, 4631−4646.
(27) Borówko, M.; Rżysko, W.; Sokołowski, S.; Staszewski, T. *J. Chem. Phys.* **2007**, *126*, 214703.
(28) Borówko, M.; Rżysko, W.; Sokołowski, S.; Staszewski, T. *J. Phys. Chem. B* **2009**, *113*, 4763−4770.
(29) Borówko, M.; Sokołowski, S.; Staszewski, T. *J. Chromatogr. A* **2011**, *1218*, 711−720.
(30) Borówko, M.; Sokołowski, S.; Staszewski, T. *J. Phys. Chem B* **2012**, *116*, 3115−3124.
(31) Borówko, M.; Sokołowski, S.; Staszewski, T. *J. Phys. Chem. B* **2012**, *116*, 12842.
(32) Borówko, M.; Patrykiejew, A.; Pizio, O.; Sokołowski, S. *Condens. Matter Phys.* **2011**, *14*, 33604.
(33) Borówko, M.; Staszewski, T. *Condens. Matter Phys.* **2012**, *15*, 23603.
(34) Xu, Y.; Chen, X.; Chen, H.; Xu, S.; Liu, H.; Hu, Y. *Mol. Simul.* **2012**, *38*, 274−284.
(35) Weinhold, J. D.; Kumar, S. K. *J. Chem. Phys.* **1994**, *101*, 4312−4323.
(36) Klatte, S. J.; Beck, T. L. *J. Phys. Chem.* **1996**, *100*, 5931−5934.
(37) Grest, G. S. *J. Chem. Phys.* **1996**, *105*, 5532−5541.
(38) Lippa, K. A.; Sander, L. C.; Mountain, R. D. *Anal. Chem.* **2005**, *77*, 7852−7861.
(39) Pastorino, C.; Binder, K.; Keer, T.; Mueller, M. *J. Chem. Phys.* **2006**, *124*, 064902.
(40) MacDowell, L. G.; Mueller, M. *J. Chem. Phys.* **2006**, *124*, 084907.
(41) Milchev, A.; Egorov, S. A.; Binder, K. *J. Chem. Phys.* **2010**, *132*, 184905.
(42) Hsu, H.-P; Paul, W.; Binder, K. *J. Chem. Phys.* **2010**, *133*, 134902.
(43) Rafferty, J. L.; Siepmann, I.; Schure, M. R. *J. Chromatogr. A* **2008**, *1204*, 11−19.
(44) Rafferty, J. L.; Siepmann, I.; Schure, M. R. *J. Chromatogr. A* **2009**, *1216*, 2320−2331.
(45) Fouqueau, A.; Meuwly, M.; Bemish, R. J. *J. Phys. Chem. B* **2007**, *111*, 10208−10216.
(46) Braun, J.; Fouqueau, A.; Bemish, R. J.; Meuwly, M. *J. Phys. Chem. Chem. Phys.* **2008**, *10*, 4765−4777.
(47) Currie, E. P. K.; Norde, W.; Coehn Stuart, M. A. *Adv. Colloid Interface Sci.* **2003**, *100*, 205−265.
(48) Netz, R. R.; Andelman, D. *Phys. Rep* **2003**, *380*, 1−95.
(49) Binder, K.; Milchev, A. *J. Polymer Sci. Polymer Phys.* **2012**, *50*, 1515−1555.
(50) Scheutjens, J. M. H. M.; Fleer, G. J. *Macromolecules* **1979**, *83*, 1619−1635.
(51) Scheutjens, J. M. H. M.; Fleer, G. J. *Macromolecules* **1980**, *84*, 178−190.
(52) Yu, Y.-X.; Wu, J. *J. Chem. Phys.* **2002**, *117*, 2368−2376, 10156−10164.
(53) Yu, Y.-X.; Wu, J. *J. Chem. Phys.* **2003**, *118*, 3835−3842.
(54) Mueller, M.; MacDowell, L. G.; Yethiraj, A. *J. Chem. Phys.* **2003**, *118*, 2929−2940.
(55) Freed, K. F. *J. Chem. Phys.* **1995**, *103*, 3230−3239.
(56) Bryk, P.; MacDowell, L. G. *J. Chem. Phys.* **2008**, *129*, 104901.
(57) Sentell, K. B. *J. Chromatogr. A* **1993**, *656*, 231−263.
(58) Sentell, K. B.; Bliesner, D. M.; Shearer, S. T. In *Chemically Modified Surface*; Pesek, J. J., Leigh, I. E., Eds.; Royal Society of Chemistry: Cambridge, 1994; p 190.
(59) Rutan, S. C.; Harris, J. M. *J. Chromatogr. A* **1993**, *656*, 197−215.
(60) Sander, L. C.; Callis, J. B.; Fielf, L. R. *Anal. Chem.* **1988**, *55*, 1068−1075.
(61) Doye, C. A.; Vickers, T. J.; Mann, C. K.; Dorsey, J. G. *J. Chromatogr. A* **2000**, *656*, 25−39.
(62) Liao, Z. H.; Pemberton, J. E. *Anal. Chem.* **2008**, *80*, 2911−2920.
(63) Dorsey, J. G.; Dill, A. K. *Chem. Rev.* **1989**, *89*, 331−346.
(64) Weeks, J. D.; Chandler, D.; Andersen, H. C. *J. Chem. Phys.* **1971**, *54*, 5237−5247.
(65) Rosenfeld, J. *Phys. Rev. Lett.* **1989**, *63*, 980−983.
(66) Wertheim, M. S. *J. Chem. Phys.* **1987**, *87*, 7323−7331.
(67) Everett, D. H. *Trans. Faraday Soc.* **1965**, *61*, 2478−2495.
(68) Ash, S. G.; Everett, D. H.; Findenegg, G. H. *Trans. Faraday Soc.* **1970**, *66*, 708−722.
(69) Roe, R.-J. *J. Chem. Phys.* **1974**, *60*, 4192−4207.
(70) Gritti, F.; Kazakevich, Y. V.; Guiochon, G. *J. Chromatogr. A* **2007**, *1169*, 111−124.
(71) Bocian, S.; Vajda, P.; Felinger, A.; Buszewski, B. *Anal. Chem.* **2009**, *81*, 6334−6346.
(72) Tchapla, A.; Colin, H.; Guiochon, G. *Anal. Chem.* **1984**, *56*, 621−625.
(73) Moh, L. C. H.; Losego, M. D.; Braun, P. V. *Langmuir* **2011**, *27*, 3698−3702.